ChemBioChem

Combining Chemistry and Biology

Chemistry Europe

European Chemical Societies Publishing

Accepted Article

Title: Salt-toggled Capture Selection of Uric Acid Binding Aptamers

Authors: Yibo Liu and Juewen Liu

To be cited as: *ChemBioChem* **2022**, e202200564

Link to VoR: https://doi.org/10.1002/cbic.202200564

WILEY-VCH

Salt-toggled Capture Selection of Uric Acid Binding Aptamers

Dr. Yibo Liu[a,b] and Prof. Juewen Liu[a,b]*

a. Department of Chemistry, Waterloo Institute for Nanotechnology, University of Waterloo, Waterloo, ON, N2L 3G1, Canada

b. Centre for Eye and Vision Research (CEVR), 17W Hong Kong Science Park, Hong Kong

Email: liujw@uwaterloo.ca

Abstract

Uric acid is the end-product of purine metabolism in humans and an important biomarker for many diseases. To achieve the detection of uric acid without using enzymes, we previously selected a DNA aptamer for uric acid with a K_d of 1 μM but the aptamer required multiple Na^+ ions for binding. Saturated binding was achieved with around 700 mM Na^+ and the binding at the physiological condition was much weaker. In this work, a new selection was performed by alternating Mg^{2+}-containing buffers with Na^+ and Li^+. After 13 rounds of selection, a new aptamer sequence named UA-Mg-1 was obtained. Isothermal titration calorimetry confirmed aptamer binding in both selection buffers, and the K_d was around 8 μM. The binding of UA-Mg-1 to UA required only Mg^{2+}. This is an indicator of successful switching of metal dependency via the salt toggled selection method. The UA-Mg-1 aptamer was engineered into a fluorescent biosensor based on the strand-displacement assay with a limit of detection of 0.5 μM uric acid in the selection buffer. Finally, a comparison with the previously reported Na^+-dependent aptamer and a xanthine/uric acid riboswitch was also made.

Keywords: aptamers; biosensors; uric acid; magnesium; SELEX

Introduction

Uric acid (UA) is endogenously produced from purine metabolism in mammals.[1] In the majority of mammals, UA is further converted to allantoin by uricase, but UA exists in high concentrations in human due to a lack of uricase.[2-3] An abnormal UA level is indicative of many diseases including gout, kidney diseases, high blood pressure, and neurodegenerative diseases.[4]

The measurement of UA can be achieved by using analytical instrumentation such as high-performance liquid chromatography-mass spectrometry.[5-6] Enzyme-based methods have also been developed, most of which will convert UA to produce H_2O_2 as a by-product. H_2O_2 can be subsequently quantified with chromogenic peroxidase substrates[7-13] or by electrochemistry.[14-16] Such methods require multiple-step cascade reactions and UA was measured indirectly.

Aptamers are single-stranded oligonucleotides that can selectively bind to target molecules. Most aptamers were isolated in vitro from randomized libraries by systematic evolution of ligands by exponential enrichment (SELEX).[17-19] They can bind to a variety of targets with excellent specificity and affinity. DNA aptamers offer many advantages in biosensing, including high stability, programmable structures, and ease of incorporation of versatile signal reporting probes.[20-21] UA, as a purine analog, may have strong interactions with DNA via π-π stacking and hydrogen bonding.

We recently isolated a UA-binding DNA aptamer that showed excellent binding affinity (K_d ~1 μM) and specificity to UA.[22] However, it was selected in a high salt buffer (1 M NaCl) and the aptamer required three Na^+ ions to achieve the binding interaction. The binding affinity saturated at around 700 mM Na^+. Thus, the binding affinity was lower in the physiological condition. Since aptamers often work the best under the condition of their selection, we wanted to see if we can obtain new aptamers that work optimally under physiological conditions. To achieve this goal, we herein performed a new selection by alternating Na^+ and Li^+ in the selection rounds, and both buffers contained 10 mM Mg^{2+}. In the end, a Mg^{2+}-dependent aptamer was isolated to bind to UA.

Experimental Section

Chemicals

The DNA oligonucleotides were obtained from Integrated DNA Technologies (Coralville, IA, USA), and their sequences are listed in **Table S1**. UA, xanthine, adenine, adenosine, caffeine, theophylline, tryptophan, guanine, and ethidium bromide were purchased from Millipore-Sigma. Agarose and L-tyrosine were from Bio Basic. Dextrose was from VWR. Tri(hydroxymethyl)aminomethane (Tris), NaCl, $MgCl_2$, KCl and LiCl were from Mandel Scientific (Guelph, Canada). SsoFast EvaGreen supermix was from New England Biolabs. Streptavidin-coated agarose resin was from Thermo Scientific (IL, USA).

SELEX procedures

The aptamer selection was carried out based on the previously described procedures with a few modifications.[23-25] The detailed procedures are described in Supporting Information.

Isothermal titration calorimetry (ITC)

ITC experiments were performed using a VP-ITC microcalorimeter instrument (MicroCal). Aptamer samples were loaded in the cell (1.45 mL, 10 μM) in buffer. UA and other molecules (280 μL of 400 μM) in the same buffer were loaded in the instrument syringe. Each titration contained 28 injections with an initial purge injection of 2 μL, 5 μL for the 2nd-10th injections, 10 μL for the 11th-20th injections, and 15 μL for the 21st to 28th injections). The titration spacing was 180s between each injection. The integrated heat of each injection was calculated. The binding constants (K_a) were obtained through fitting the titration curves to a one-site binding model using the Origin software. The dissociation constant (K_d) values were calculated from taking the reciprocal of K_a.

Aptamer-based biosensor assays

One micromolar sensor (aptamer/quencher complex) was prepared by annealing 1 μM FAM-labeled UA-Mg-1 aptamer with 2 μM quencher-cDNA in the selection buffer at 80 °C for 1 min, followed by cooling to room temperature over 20 min and then at 4°C for 1 h. Afterwards, the sensor was stored at -20 °C prior to use. In a typical experiment, 100 μL sample containing 20 nM of sensors was used. The background fluorescence of the sensor was monitored for 5 min. Then 2 μL of target solution was added. The fluorescence signal was continuously monitored for another 15 min (Ex: 495 nm, Em: 525 nm) with 20 s intervals. The experiments were run in triplicate and graphed with error bars to indicate the standard deviations.

Results and Discussion

Salt-toggled SELEX

The aptamer selection was performed using the library-immobilization method.[24, 26-27] A scheme of the selection is shown in Scheme 1. A 73-nt DNA library containing a 30-nucleotide (nt) random region (N_{30}) flanked by two constant primer-binding regions was immobilized on streptavidin-coated agarose column via hybridization with an 18-nt biotinylated column-binding strand. The library sequence was designed to form a hairpin structure, which was opened by the column-binding strand. Upon binding with UA, the hairpin is formed and the strand is released from the column, collected, and amplified for next round of selection. Our previously selected aptamer requires a high Na^+ concentration for binding.[22] To suppress Na^+-dependent binding, we reduced the NaCl concentration from 1 M to 150 mM which is close to the

physiological condition. In addition, we toggled the selection by alternating buffers containing Na^+ and Li^+ (Table S2) between each round. Both buffers contained 10 mM Mg^{2+}.

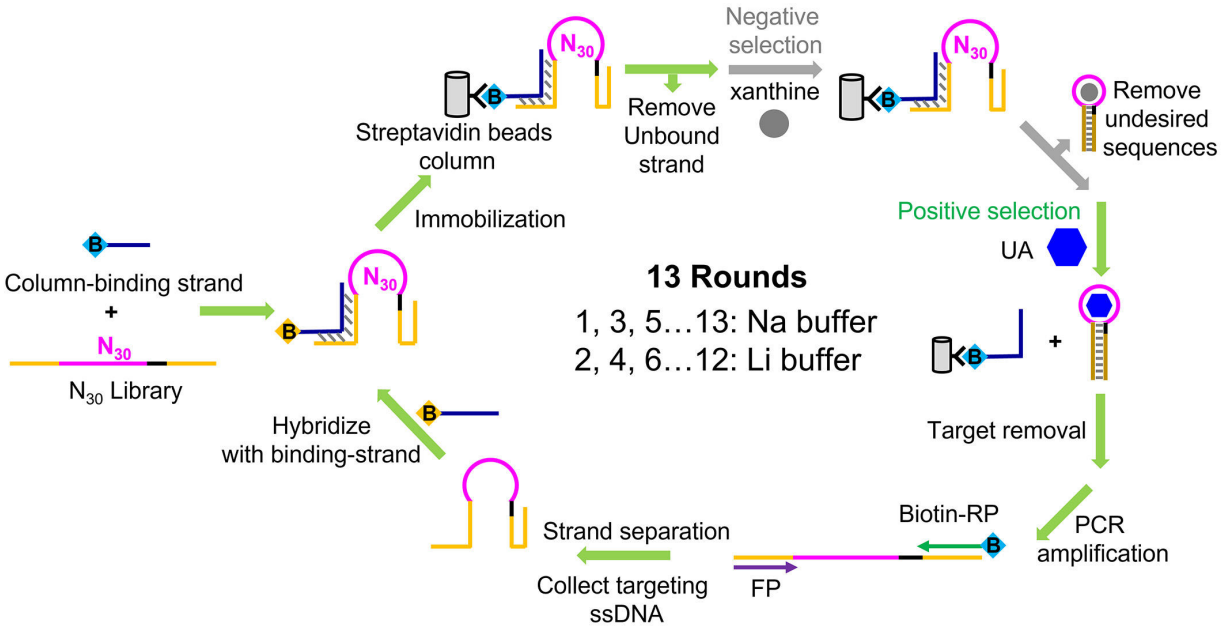

Scheme 1. A scheme of the salt-toggled SELEX. The Na^+ buffer contained 150 mM NaCl, while the Li^+ buffer contained 150 mM LiCl. Both buffers contained 20 mM Tris, pH 8.3, 10 mM $MgCl_2$ and 10 mM KCl.

New UA binding aptamers

A total of 13 rounds of selection were performed. The initial UA concentration was 5 mM, which was gradually decreased to 0.2 mM (Table S3) to increase the selection stringency. From round 8, we introduced a counter selection step using xanthine to improve binding specificity (Scheme 1), since xanthine differs from UA by only a single oxygen atom. The round 13 library was deep sequenced. A total of 44,947 sequences were obtained and assigned to 461 groups by the Geneious software. Since all the sequences can fold to a hairpin structure, we truncated the primer binding regions and kept five base pairs to produce 40-nt aptamers. The first 20 most abundant sequences were aligned using Clustal Omega, which were grouped into three families along with some unclassified sequences (Figure 1a). Out of the three families, two contained the same conserved sequences by flipped sides. Similar circular permutation binding regions were also observed in the previous UA aptamer selection,[22] and other selections.[28-30] The majority of the sequences belonged to Family 1. These sequences contain a hairpin structure (the blue/black regions in Figure 1a), while the orange regions are conserved nucleotides. The conserved regions in Family 1 are rich

in purines, and the most abundant sequence was named UA-Mg-1, which can fold to a well-defined structure (Figure 1b). Family 3 contained the same previous Na^+-dependent aptamers. Figure 1c shows the structure of our previous UA aptamer named UA-1,[22] and in this work we renamed it to UA-Na-1.

UA-Na-1 was the most abundant sequence in our previous selection, but here this exact sequence was not in the top 20, suggesting that the Family 3 sequences were from our current selection instead of contamination from the previous selection. Even though we used a lower concentration of Na^+ and also used Na^+-free buffers, UA-Na-1 like sequences still survived. It is not surprising that they can also bind UA at low Na^+ conditions, although with lower affinities. Among the unclassified sequences, a few also share the feature of containing purine-rich regions (in orange) and some with a stretch of pyrimidines (in red). Since these sequences are less representative, they were not analyzed further here.

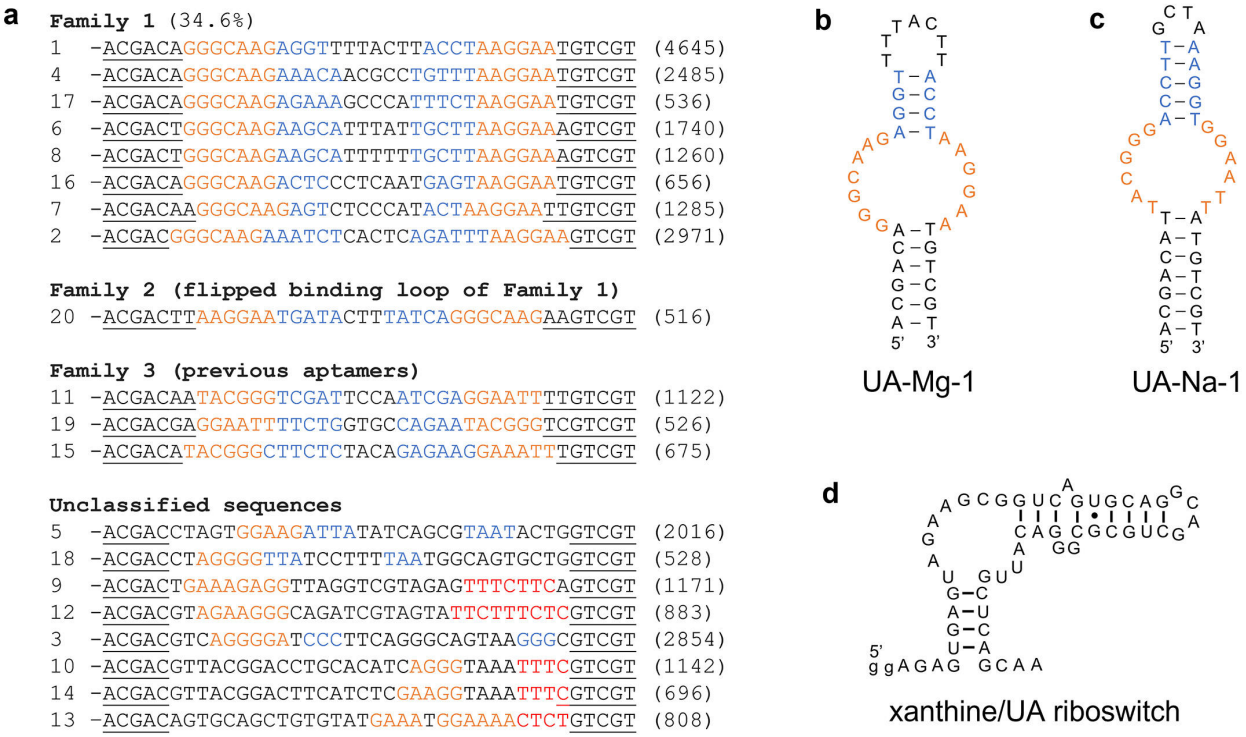

Figure 1. (a) Sequence alignment of the top 20 sequences from the current salt-toggled UA selection. The secondary structures of the newly selected aptamer (UA-Mg-1), and (c) the previous aptamer that we re-named it UA-Na-1 here. The underlined regions base pair. (d) The secondary structure of the aptamer region from a xanthine/UA riboswitch.[31]

Salt-dependent UA binding

To test whether the obtained sequences can bind UA, we used isothermal titration calorimetry (ITC). The Mfold[32] predicted secondary structure of the UA-Mg-1 aptamer is shown in Figure 1b. First, we tested the binding of UA-Mg-1 in the two selection buffers. Figure 2a shows the thermogram and integrated heat in the Na^+ selection buffer, and the fitted K_d value was 7.3 μM. Figure 2b shows the data in the Li^+ selection buffer, and the fitted K_d was 8.1 μM. Their comparable K_d values indicated the binding of UA-Mg-1 with UA is independent of either metal ion.

We then further tested the metal dependency by removing Na^+ from the buffer but keeping the same Mg^{2+} concentration. As shown in Figure 2c, a K_d of 5.2 μM UA was obtained, which is close to the binding in the selection buffer (Figure 2a and 2b), further indicating that the binding is independent of Na^+. We also removed K^+ from the Mg^{2+}-containing buffer, and a similar K_d of 5.1 μM was obtained (Figure S1a), demonstrating K^+ was not involved in the binding. When we kept 150 mM Na^+ but removed Mg^{2+} from the buffer, no binding was observed (Figure 2d). The replacement of Mg^{2+} by Ca^{2+} also weakened the binding with a fitted K_d of 25.4 μM (Figure S1b). Therefore, Mg^{2+} is required for binding. The ITC results demonstrated that we successfully switched the metal ion-dependency by altering the selection conditions.

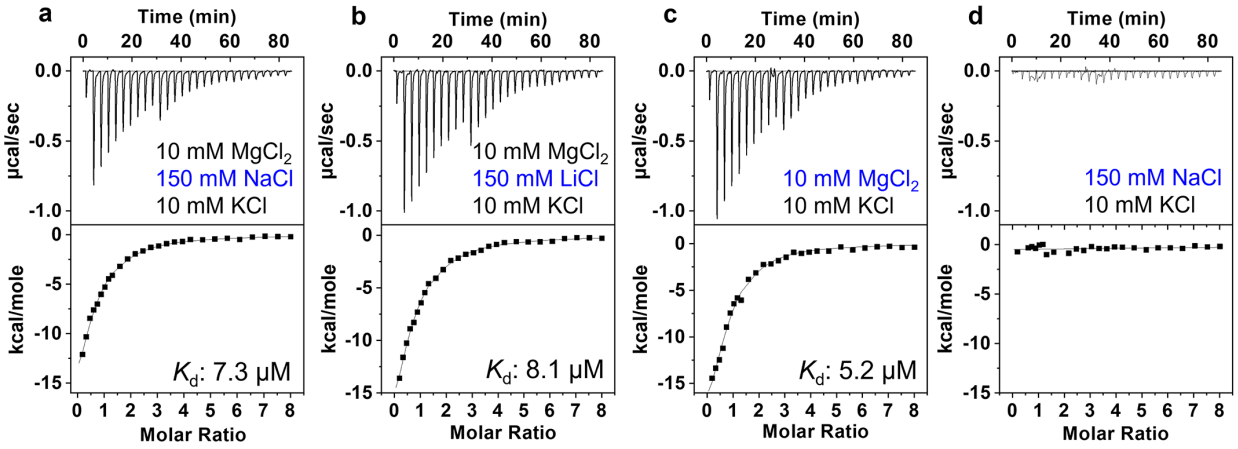

Figure 2. The ITC traces and integrated heat of titrating UA (400 μM) to UA-Mg-1 (10 μM) in (a) the Na buffer (20 mM Tris, pH 8.3, 10 mM KCl, 10 mM $MgCl_2$, and 150 mM NaCl), (b) the Li buffer (20 mM Tris pH 8.3, 10 mM KCl, 10 mM $MgCl_2$, and 150 mM LiCl), (c) without Na^+/Li^+ (20 mM Tris, pH 8.3, 10 mM KCl, and 10 mM $MgCl_2$), and (d) without Mg^{2+} (20 mM Tris pH 8.3, 10 mM KCl, and 150 mM NaCl).

We then varied the Mg^{2+} concentration in the buffer (20 mM Tris, 150 mM NaCl, 10 mM KCl, with different concentration of Mg^{2+}). As shown in Figure 3, the binding increased with increasing Mg^{2+} concentration. We then compared the thermodynamic values of the previous Na^+-dependent aptamers and the current Mg^{2+}-dependent aptamers (Table 1). When UA was titrated to UA-Na-1 the ΔH of the reaction was -21

kcal mol^{-1}, whereas the Δ*H* was -31 kcal mol^{-1} for UA-Mg-1. The amount of heat released by UA-Mg-1 was larger, and Mg^{2+} might be responsible for the increased heat released (e.g. by forming a salt bridge). The Δ*S* for titrating UA to UA-Na-1 was -43.8 cal mol^{-1} K^{-1}, and the Δ*S* for titrating to UA-Mg-1 was -79.0 cal mol^{-1} K^{-1}. In the case of the Mg^{2+}-mediated binding, the system had much lower entropy in the UA bound state. The forming of Mg^{2+}-bridged interactions likely decreased the flexibility of the binding complex.

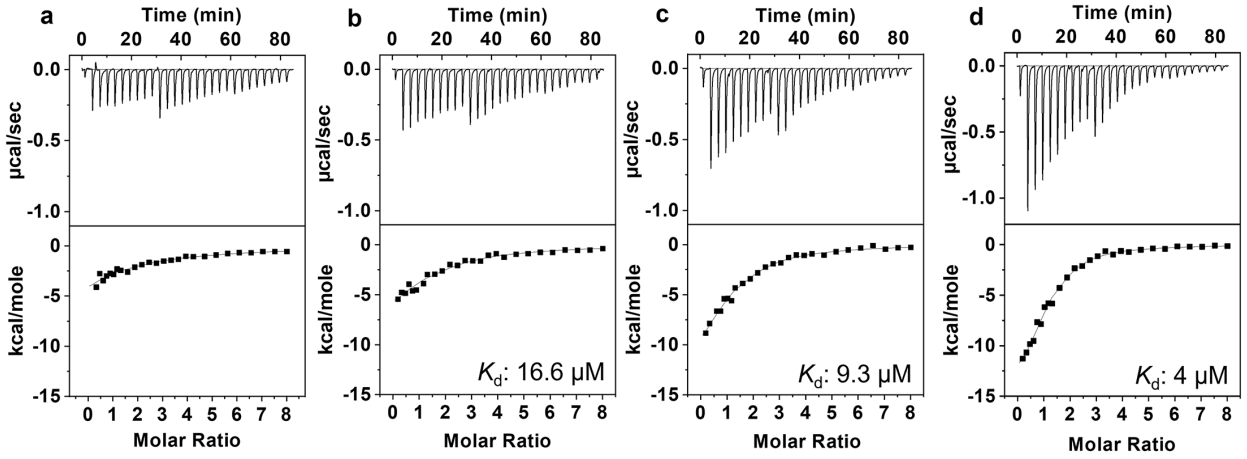

Figure 3. ITC curves and integrated heat of titrating UA (400 µM) to UA-Mg-1 (10 µM) in buffer containing (a) 1 mM, (b) 2 mM, (c) 5 mM and (d) 20 mM Mg^{2+}.

Table 1. Thermodynamic data for titrating UA to the UA-Na-1 and UA-Mg-1 aptamers in their respective selection buffers (1 M NaCl and 10 mM Mg^{2+} for UA-Na-1; and 150 mM NaCl and 10 mM Mg^{2+} for UA-Mg-1).

Thermodynamic values	**UA-Na-1**	**UA-Mg-1**
K_a (× 10^5 M^{-1})	7.5 ± 1.4	1.4 ± 0.1
Δ*H* (kcal mol^{-1})	-21 ± 1	-31 ± 4
Δ*S* (cal mol^{-1} K^{-1})	-43.8	-79.0
Δ*G* (kcal mol^{-1})	-8.0 ± 1.1	-7.1 ± 3.5
N	0.80 ± 0.03	0.60 ± 0.06

Fluorescent sensing of UA

To further evaluate the binding property of this aptamer, we used the strand displacement assay,[24, 33] which can also be used as a fluorescent biosensor for UA. We extended the UA-Mg-1 aptamer strand by a few nucleotides and labeled it with a FAM fluorophore. This strand was then hybridized with a quencher-labeled short complementary strand, resulting in quenched fluorescence. Upon target binding, the quencher strand is displaced which restores the fluorescence signal. Initially, we varied the Mg^{2+} concentration in the buffer using 20 nM sensor. As shown in Figure 4a, with the increase of Mg^{2+} concentration, the background signal was lowered, and the signal response was larger. A lower background fluorescence can be attributed to improved hybridization with the quencher-labeled strand, and a higher signal can be attributed to better aptamer binding. Thus, a higher Mg^{2+} concentration gave a better signal-to-background ratio. By fitting the signal change over Mg^{2+} concentration, a Hill coefficient of 0.59 ± 0.08 was obtained (Figure 4b). Based on the shape of a normal binding curve, we reason that only one Mg^{2+} ion was involved in the binding reaction. This is in sharp contrast to a Hill coefficient of 2.8 from the UA-Na-1 sensor.[22] Thus, UA-Mg-1 likely uses one Mg^{2+} ion to binding UA, whereas UA-Na-1 uses three Na^{+} ions to achieve the same goal (Figure 4e).

After understanding the effect of Mg^{2+}, we then tested its response to UA in the selection buffer (the Na^{+} buffer). Different concentrations of UA (1 μM to 200 μM) were added, and the fluorescence change is shown in Figure 4c. By fitting the data, an apparent K_d of 8.9 μM was obtained. This is similar to the K_d obtained from ITC, suggesting that the competition from the quencher-labeled strand was low.[34] This can also be seen from the high background fluorescence, which in turn resulted in a saturated fluorescence enhancement of just below 1-fold. The weak competition also led to fast signaling kinetics, where a stable signal was achieved in ~1 min at high UA concentrations. For comparison, in the recently reported oxytetracycline aptamer, the fluorescence enhancement reached ~20-fold, but the apparent K_d from the sensor (12 μM) was 80-fold higher than the real K_d of the aptamer (0.15 μM).[35] As a result, the limit of detection (LOD) for oxytetracycline was 1.2 μM, which is eight times higher than the K_d of the aptamer. The LOD for the UA sensor was calculated to be 0.5 μM UA based on 3σ/slope, which was 10-fold below the K_d value of the aptamer (5.2 μM).

10.1002/cbic.202200564

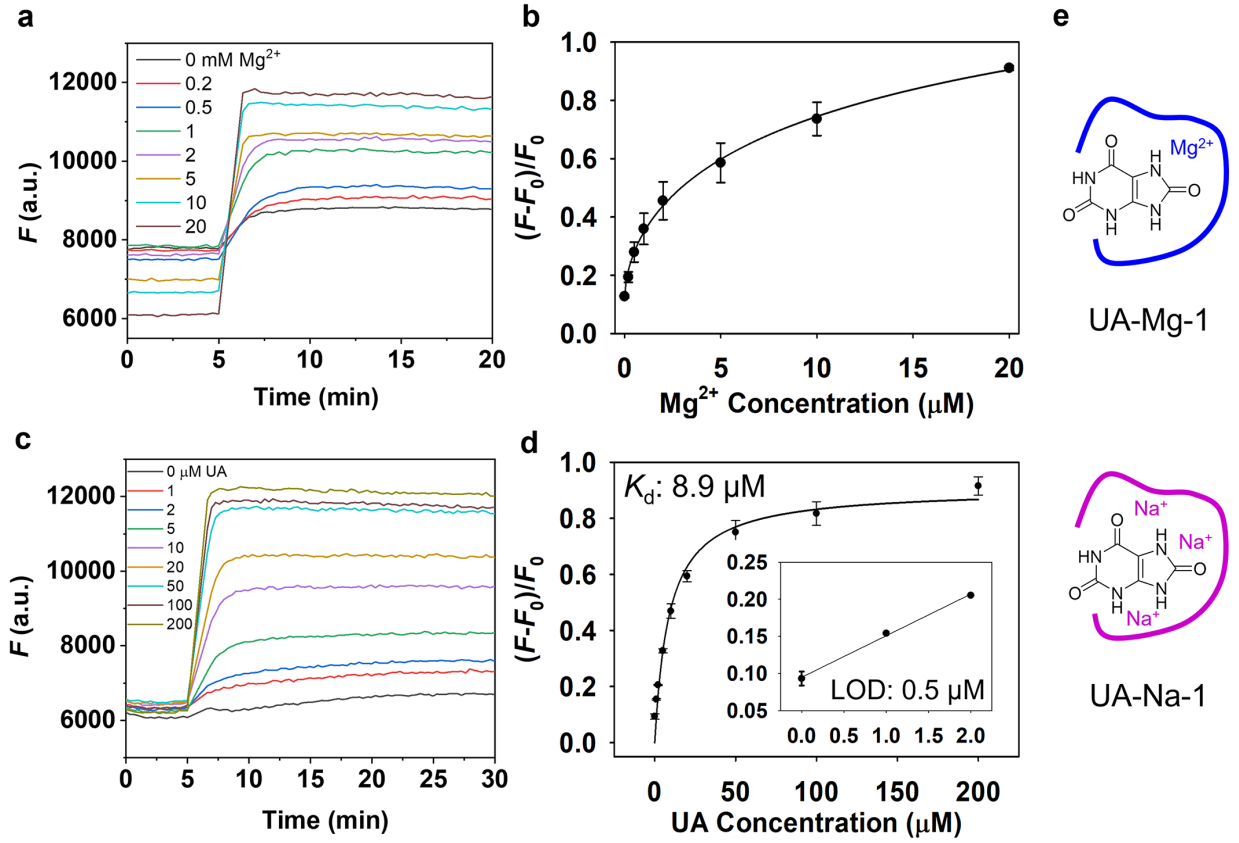

Figure 4. (a) Response of the sensor to 100 μM UA in the presence of different concentration of Mg^{2+}. (b) Fluorescence response as a function of Mg^{2+} concentration. (c) Fluorescence enhancement of the sensor to various concentration of UA in the Na^{+} selection buffer. (d) Calibration curve of the sensor. Inset: the linear response at low UA concentrations. (e) A cartoon showing the need of one Mg^{2+} by UA-Mg-1 and three Na^{+} ions by UA-Na-1.

We then tested the selectivity of the UA-Mg-1 sensor against several biomolecules structural similar to UA. As shown in Figure 5, UA-Mg-1 had no response to most of them except for xanthine. Although we performed negative selections using xanthine, the cross-activity with xanthine still cannot be eliminated. Figure 5 also shows the structures of UA and xanthine, and they differed only by a single oxygen atom. Although the selectivity was only about one-fold, the physiological UA concentration is in the hundreds of micromolar range,[15, 36] but the xanthine concentration was less than several micromolar.[37] Therefore practically, xanthine is unlikely to interfere with the detection of UA when using this aptamer.

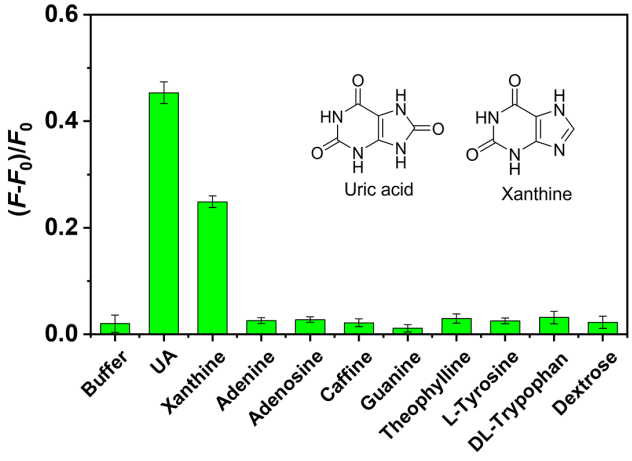

Figure 5. The selectivity of the UA-Mg-1 sensor against various structural similar molecules (20 μM). The chemical structures of UA and xanthine are shown.

Comparison with the UA-Na-1 aptamer

It is interesting that two aptamers for the same target had a very similar secondary structure (Figure 1b, c), but completely different metal requirements. We checked sequences in each other's sequencing pool and found that the previously obtained UA-Na-1 family (with the same conserved sequences) represented 12% of the current selection pool (Table 2). This number, although lower than the UA-Mg-1 family (34.6%), still makes up a significant portion of the final pool. In contrast, the UA-Mg-1 family was present at only 2.2% in the previous selection. Therefore, in principle, if we tested sufficient sequences in our previous selection for their metal requirement, we can eventually find UA-Mg-1 without doing a new selection. The use of mixed metals in our previous buffer (Na^+ and Mg^{2+}) may explain the selection results. The K_d values the under selection conditions for UA-Na-1 and UA-Mg-1 are 1 μM and 7-8 μM, respectively. The higher K_d of UA-Mg-1 may also contribute to its lower abundance in the previous selection.

UA-Mg-1 and UA-Na-1 have similar secondary structure but different conserved sequences. Both UA-Na-1 and UA-Mg-1 contain two loops linked by a hairpin. UA-Mg-1 has conserved sequences of GGGCAAG and AAGGAA in the loop region, while UA-Na-1 has conserved sequences of TACGGG and GGAATT. The investigation of how these minor changes in the conserved sequences govern the metal preference will be a topic of future studies, which will require high resolution structural biology methods such as NMR or X-ray crystallography. Finally, both of the aptamers have strong cross activity with xanthine. UA-Na-1 was obtained without negative selection, while UA-Mg-1 was obtained with extensive negative selection. Yet, they had similar selectivity for UA over xanthine. It is likely that a single oxygen at that particular position

can be quite difficult for DNA aptamers. In other examples, such as theophylline and caffeine, a single method group can bring in over 10,000 to 250,000 fold selectivity.[28-29]

The switch of metal ion-dependency by changing buffer was also reported by Szostak.[38] When the RNA aptamers for cyanocobalamin (vitamin B12) were selected in the selection buffer containing 1 M Li^+ and 5 mM Mg^{2+}, the binding required Li^+, which cannot be substituted by Na^+ or K^+ even with the presence of Mg^{2+}. Whereas the selection buffer containing 1 M NaCl and 5 mM $MgCl_2$ was used, the metal ion-dependency could be switched to Na^+/K^+ plus Mg^{2+}.[38] A few toggled SELEX were reported previously.[39-42] For example, Sullenger's group selected RNA aptamers that recognize both human and porcine thrombin by alternating the protein targets (human and porcine thrombin) in each round.[39] The selection of RNA aptamers for aminoglycoside antibiotics was carried out by alternating between two structurally related aminoglycosides, resulting in sequences that can recognize conserved structural features of the aminoglycoside pair.[42] Most of the selection used toggled targets to increase the cross-activity of structural similar compounds. Herein we toggled the selection buffers to switch the metal dependency.[43]

Comparison with the xanthine/uric acid riboswitch

From many orphan riboswitch candidates, Yu and Breaker identified the MNT1 motif containing a small aptamer structure that can bind to xanthine and UA.[31] Using the in-line probing method, one of the MNT1 containing sequences (Figure 1d) showed a K_d of ~3.7 μM xanthine and ~25 μM UA. In this case, the selectivity between these two molecules were about 7-fold, which was similar to what we observed in UA-Na-1.[22] In the in-line probing assay, 100 mM K^+ and 20 mM Mg^{2+} were added. So, we tend to believe that MNT1 is an Mg^{2+}-dependent aptamer, although no detailed metal-dependent studies were performed. In our two UA binding aptamers, the UA had better affinity than xanthine, since we used UA as the selection target. Had xanthine been used as the target, we might have obtained aptamers that are more selective for xanthine. The structure of the xanthine riboswitch aptamer is also a two-way junction, which was similar to our UA DNA aptamers. One of the unpaired loops of the riboswitch aptamer is rich in purines, while our UA DNA aptamers are rich in purines in both loops. The similar overall secondary structures and purine-rich loops suggested that the riboswitch and our aptamers might have a similar way of binding.

Table 2. The comparison of UA-Mg-1 and UA-Na-1

Aptamers	UA-Mg-1	UA-Na-1
Percentage in its own pool	34.6 (round 13)	56.7 (round 18)
Percentage found in the other pool	2.2 (round 18)	12 (round 13)

Consensus sequences in loop	GGGCAAG/AAGGAA	TACGGG/GGAATT
Metal ion dependency	saturated at 10 mM Mg^{2+}	saturated at 700 mM Na^{+}
K_d under selection conditions	7-8 μM	1 μM

Conclusions

In this work, we selected a new UA binding aptamer by alternating the buffers containing Na^{+} and Li^{+}. After 13 rounds selection, UA-Mg-1 was obtained with Mg^{2+}-dependent binding to UA. The aptamer had a similar secondary structure to UA-Na-1, which required a high concentration of Na^{+} for UA binding (no Mg^{2+} requirement). These two aptamers have very similar secondary structures and only differ by a few nucleotides in the binding loops. Yet, they have completely different metal requirements. The binding of UA-Mg-1 to UA was confirmed by ITC in both Na^{+} and Li^{+} selection buffers with comparable K_d of around 8 μM. In addition, a fluorescent biosensor for UA was developed based on the strand-displacement assay in the selection buffer and a limit of detection of 0.5 μM UA was obtained. So far, two aptamers were obtained that can be used for UA sensing and this might find applications in the bioanalysis of UA as a biomarker.

Acknowledgements

Funding for this work was from the Hong Kong Special Administrative Region Government and InnoHK and the Natural Sciences and Engineering Research Council of Canada (NSERC).

Keywords: biosensors, DNA aptamers, metal ion, SELEX, uric acid

Conflict of Interest

The authors declare no conflict of interest.

References

[1] S. E. Liebman, J. G. Taylor, D. A. Bushinsky, *Curr. Rheumatol Rep.* **2007**, *9*, 251-257.
[2] Y. Y. Sautin, R. J. Johnson, *Nucleosides, Nucleotides, Nucleic Acids* **2008**, *27*, 608-619.
[3] B. Álvarez-Lario, J. Macarrón-Vicente, *Rheumatology* **2010**, *49*, 2010-2015.
[4] E. P. d. Oliveira, R. C. Burini, *Diabetol. Metab. Syndr.* **2012**, *4*, 12.
[5] X. Dai, X. Fang, C. Zhang, R. Xu, B. Xu, *J. Chromatogr. B* **2007**, *857*, 287-295.
[6] Q. Wang, X. Wen, J. Kong, *Crit. Rev. Anal. Chem.* **2020**, *50*, 359-375.

[7] N. E. Azmi, N. I. Ramli, J. Abdullah, M. A. A. Hamid, H. Sidek, S. A. Rahman, N. Ariffin, N. A. Yusof, *Biosens. Bioelectron.* **2015**, *67*, 129-133.
[8] A. Fang, Q. Wu, Q. Lu, H. Chen, H. Li, M. Liu, Y. Zhang, S. Yao, *Biosens. Bioelectron.* **2016**, *86*, 664-670.
[9] Y. He, F. Qi, X. Niu, W. Zhang, X. Zhang, J. Pan, *Anal. Chim. Acta* **2018**, *1021*, 113-120.
[10] J. Wang, X. Fang, Y. Zhang, X. Cui, H. Zhao, X. Li, Z. Li, *Colloids Surf., A* **2018**, *555*, 565-571.
[11] C. Xiong, T. Zhang, W. Kong, Z. Zhang, H. Qu, W. Chen, Y. Wang, L. Luo, L. Zheng, *Biosens. Bioelectron.* **2018**, *101*, 21-28.
[12] F. Yang, Z. Yu, X. Li, P. Ren, G. Liu, Y. Song, J. Wang, *Spectrochim. Acta, Part A* **2018**, *203*, 461-471.
[13] X. Wang, Q. Yao, X. Tang, H. Zhong, P. Qiu, X. Wang, *Anal. Bioanal. Chem.* **2019**, *411*, 943-952.
[14] D. Lakshmi, M. J. Whitcombe, F. Davis, P. S. Sharma, B. B. Prasad, *Electroanalysis* **2011**, *23*, 305-320.
[15] B. Thakur, S. N. Sawant, *ChemPlusChem* **2013**, *78*, 166-174.
[16] B. Peng, J. Cui, Y. Wang, J. Liu, H. Zheng, L. Jin, X. Zhang, Y. Zhang, Y. Wu, *Nanoscale* **2018**, *10*, 1939-1945.
[17] A. D. Ellington, J. W. Szostak, *Nature* **1990**, *346*, 818-822.
[18] G. Tuerk, L. Gold, *Science* **1990**, *249*, 505-510.
[19] D. Wu, C. K. L. Gordon, J. H. Shin, M. Eisenstein, H. T. Soh, *Acc. Chem. Res.* **2022**, *55*, 685-695.
[20] E. J. Cho, J.-W. Lee, A. D. Ellington, *Annu. Rev. Anal. Chem.* **2009**, *2*, 241-264.
[21] M. R. Dunn, R. M. Jimenez, J. C. Chaput, *Nat. Rev. Chem.* **2017**, *1*, 0076.
[22] Y. Liu, J. Liu, *Anal. Sens.* **2022**, *2*, e202200010.
[23] K.-A. Yang, M. Barbu, M. Halim, P. Pallavi, B. Kim, D. M. Kolpashchikov, S. Pecic, S. Taylor, T. S. Worgall, M. N. Stojanovic, *Nat. Chem.* **2014**, *6*, 1003-1008.
[24] N. Nakatsuka, K.-A. Yang, J. M. Abendroth, K. M. Cheung, X. Xu, H. Yang, C. Zhao, B. Zhu, Y. S. Rim, Y. Yang, P. S. Weiss, M. N. Stojanović, A. M. Andrews, *Science* **2018**, *362*, 319-324.
[25] H. Yu, Y. Luo, O. Alkhamis, J. Canoura, B. Yu, Y. Xiao, *Anal. Chem.* **2021**, *93*, 3172-3180.
[26] R. Nutiu, Y. Li, *Angew. Chem. Int. Ed.* **2005**, *44*, 1061-1065.
[27] K.-A. Yang, H. Chun, Y. Zhang, S. Pecic, N. Nakatsuka, A. M. Andrews, T. S. Worgall, M. N. Stojanovic, *ACS Chem. Biol.* **2017**, *12*, 3103-3112.
[28] R. D. Jenison, S. C. Gill, A. Pardi, B. Polisky, *Science* **1994**, *263*, 1425-1429.
[29] P.-J. J. Huang, J. Liu, *ACS Chem. Biol.* **2022**, *17*, 2121-2129.
[30] J. P. Tobia, P.-J. J. Huang, R. S. Narayan, A. Narayan, J. Liu, *ChemRxiv* **2022**, DOI: 10.26434/chemrxiv-22022-26427gqn.
[31] D. Yu, R. R. Breaker, *RNA* **2020**, *26*, 960-968.
[32] M. Zuker, *Nucleic Acids Res.* **2003**, *31*, 3406-3415.
[33] R. Nutiu, Y. Li, *J. Am. Chem. Soc.* **2003**, *125*, 4771-4778.
[34] J. Hu, C. J. Easley, *Analyst* **2011**, *136*, 3461-3468.
[35] Y. Zhao, S. Ong, Y. Chen, P.-J. J. Huang, J. Liu, *Anal. Chem.* **2022**, *94*, 10175-10182.
[36] V. Narasimhan, R. H. Siddique, H. Park, H. Choo, *ACS Omega* **2020**, *5*, 12915-12922.
[37] N. Cooper, R. Khosravan, C. Erdmann, J. Fiene, J. W. Lee, *J. Chromatogr. B* **2006**, *837*, 1-10.
[38] J. R. Lorsch, J. W. Szostak, *Biochemistry* **1994**, *33*, 973-982.
[39] R. White, C. Rusconi, E. Scardino, A. Wolberg, J. Lawson, M. Hoffman, B. Sullenger, *Mol. Ther.* **2001**, *4*, 567-573.
[40] M. Y. Song, D. Nguyen, S. W. Hong, B. C. Kim, *Sci Rep* **2017**, *7*, 43641.
[41] B. P. Gray, L. Kelly, D. P. Ahrens, A. P. Barry, C. Kratschmer, M. Levy, B. A. Sullenger, *Proc. Natl. Acad. Sci. U. S. A.* **2018**, *115*, 4761-4766.
[42] N. Derbyshire, S. J. White, D. H. J. Bunka, L. Song, S. Stead, J. Tarbin, M. Sharman, D. Zhou, P. G. Stockley, *Anal. Chem.* **2012**, *84*, 6595-6602.

[43] W. Yang, H. Yu, O. Alkhamis, Y. Liu, J. Canoura, F. Fu, Y. Xiao, *Nucleic Acids Res.* **2019**, *47*, e71.

Table of Content

A uric acid (UA)-binding DNA aptamer was obtained using a salt toggled selection. Its binds UA with one Mg^{2+} ion, whereas a previously reported UA aptamer requires three Na^{+} ions. A fluorescence biosensor was designed based on the strand displacement assay with a limit of detection of 0.5 μM UA.

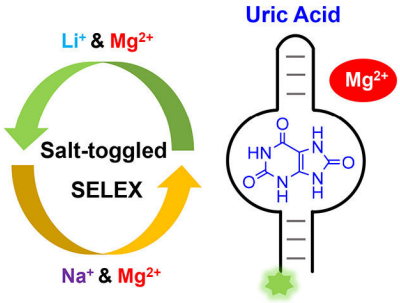

Twitter:

Juewen Liu @bionaloo

Department of Chemistry @uWaterlooChem